



LAWRENCE
LIVERMORE
NATIONAL
LABORATORY

LLNL-CONF-693020

The Design of the Optical Thomson Scattering Diagnostic for the National Ignition Facility

P. Datte, J. S. Ross, D. Froula, S. Glenzer, B. Hatch, J. Kilkenny, O. Landen, D. Manha, W. Molander, D. Montgomery, J. Moody, G. Swadling, J. Weaver

May 26, 2016

High-Temperature Plasma Diagnostics Conference
Madison, WI, United States
June 5, 2016 through June 9, 2016

Disclaimer

This document was prepared as an account of work sponsored by an agency of the United States government. Neither the United States government nor Lawrence Livermore National Security, LLC, nor any of their employees makes any warranty, expressed or implied, or assumes any legal liability or responsibility for the accuracy, completeness, or usefulness of any information, apparatus, product, or process disclosed, or represents that its use would not infringe privately owned rights. Reference herein to any specific commercial product, process, or service by trade name, trademark, manufacturer, or otherwise does not necessarily constitute or imply its endorsement, recommendation, or favoring by the United States government or Lawrence Livermore National Security, LLC. The views and opinions of authors expressed herein do not necessarily state or reflect those of the United States government or Lawrence Livermore National Security, LLC, and shall not be used for advertising or product endorsement purposes.

The design of the optical Thomson scattering diagnostic for the National Ignition Facility^{a)}

P. S. Datté^{1, b)}, J. S. Ross¹, D. H. Froula², K. D. Daub¹, J. Galbraith¹, S. Glenzer⁵, B. Hatch¹, J. Katz², J. Kilkenny¹, O. Landen¹, D. Manha¹, A. M. Manuel¹, W. Molander¹, D. Montgomery³, J. Moody¹, G. F. Swadling¹, and J. Weaver⁴

¹Lawrence Livermore National Laboratory, Livermore, California, USA

²Laboratory for Laser Energetics, University of Rochester, Rochester, New York, USA

³Los Alamos National Laboratory, Los Alamos, New Mexico, USA

⁴Plasma Physics Division, Naval Research Laboratory, Washington DC, USA

⁵SLAC National Accelerator Laboratory, Menlo Park, California, USA

The National Ignition Facility (NIF) is a 192 laser beam facility designed to support the Stockpile Stewardship, High Energy Density and Inertial Confinement Fusion programs. We report on the design of an Optical Thomson Scattering (OTS) diagnostic that has the potential to transform the community's understanding of NIF hohlraum physics by providing first principle, local, time-resolved measurements of under-dense plasma conditions. The system design allows operation with different probe laser wavelengths by manual selection of the appropriate beamsplitter and gratings before the shot. A deep-UV probe beam (λ_0 -210 nm) will be used to optimize the scattered signal for plasma densities of 5×10^{20} electrons/cm³ while a 3ω probe will be used for experiments investigating lower density plasmas of 1×10^{19} electrons/cm³. We report the phase I design of a two phase design strategy. Phase I includes the OTS telescope, spectrometer and streak camera; these will be used to assess the background levels at NIF. Phase II will include the design and installation of a probe laser.

I. INTRODUCTION

A Diagnostic Instrument Manipulator (DIM) based optical Thomson scattering diagnostic (OTS) is being designed for operation at the National Ignition Facility (NIF) to characterize under-dense plasmas^{1,2,3}. The diagnostic is being built to characterize plasma conditions present in ICF hohlraums. This information is critical to understand crossed-beam energy transfer, hohlraum wall motion and wall-hohlraum/gas-fill mix, all of which can greatly impact symmetry control and implosion performance. Detailed characterization can also be used to better understand heat transport and high-Z atomic physics which are often challenging to model. Typical gas-filled hohlraums have densities of 5×10^{20} electrons/cm³ to 5×10^{21} electrons/cm³ and temperatures of 2.5 to 5 keV. At the collection angle of ~ 11 degrees, operating in the collective scattering regime, the scattered signal collected by the diagnostic is expected to be on the order of a hundred nano-joules for a 10J probe at 5ω . In this regime, scattering from the blue shifted electron plasma wave (EPW) feature will allow us to characterize both the electron temperature and density. The ion acoustic wave (IAW) feature will be used to measure the plasma flow velocity and the ion temperature. The system is designed to measure density to within 20% and the temperature to 25%; this accuracy is primarily limited by the expected hohlraum background. Background sources, including stimulated scattering from the drive beams, Thomson scattering of the 3ω drive beams, and bremsstrahlung emission from the hot hohlraum plasma have driven the choice of the probe beam wavelength to 210 nm (5ω). The system is

focused on the blue shifted EPW resonance. We expect the red shifted peak to be unresolvable over the background produced by the 3ω drive beams. One peak should be sufficient for an accurate fit and measurement⁴.

The OTS diagnostic will be inserted into the target chamber by a DIM which requires it to have a compact design, see figure 1. The system includes a blast window, an unobscured collection telescope, transport and focusing optics, two crossed Czerny-Turner spectrometers and a shared optical streak camera photocathode, located inside of an airbox. The collection telescope is an off-axis Schwarzschild design that relays a 50 μ m spot (Thomson volume) to the shared entrance pinhole of the spectrometers⁵. A high resolution, narrow band spectrometer (0.58 meter, 2400 gr/mm) will measure the ion acoustic wave feature (e.g. 206-214 nm for a 5ω probe laser) while a low resolution, broadband spectrometer (0.14 meter, 1200 gr/mm) will measure a 50 nm band of the electron plasma wave feature. The EPW spectrometer band center wavelength will be tunable from 150-400 nm, and the IAW center wavelength is nominally fixed with only a small range of adjustability. The outputs of the spectrometers are relayed to a gated optical streak camera⁶ with selectable sweep windows between 3 and 45 ns. The inherent optical path delay between the two spectrometer systems allow the output signals to be superimposed on the same photocathode separated by approximately 5 ns. The sweep window is selected so that the required temporal resolution is achieved over the complete Thomson recording window established by the probe laser temporal pulse shape (1-5 ns). We report on the current design and expected performance at NIF.

^{a)}Contributed paper published as part of the Proceedings of the 21st Topical Conference on High-Temperature Plasma Diagnostics (HTPD 2016) in Madison, Wisconsin, USA.

^{b)}Author to whom correspondence should be addressed: datté1@llnl.gov.

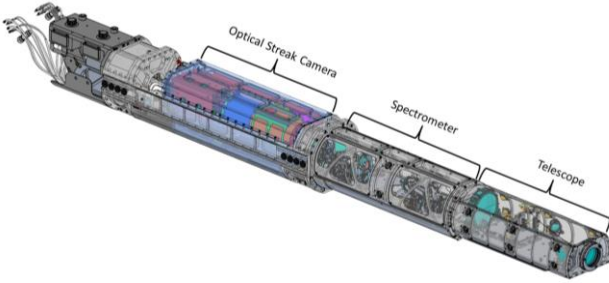


FIG. 1 The OTS diagnostic load package (DLP) configured for use in the Diagnostic Instrument Manipulators (DIM) on NIF.

II. OPTICAL DESIGN

The optical design is separated into two major sections, the telescope and the spectrometers. Following the spectrometers is the airbox assembly containing the optical streak camera. The system has been described previously and only a summary will be discussed⁷.

A. Telescope System

The telescope consists of an off-axis Schwarzschild design of 9.8° allowing an unobstructed view of the targets. The f/8.3 collection optics is the fastest system possible while still maintaining the temporal resolution requirement of 200 ps set by the relationship between the grating illumination of the IAW spectrometer and the telescope focal length⁸. An off-axis parabolic mirror focuses the collimated light onto a pinhole that defines the entrance aperture for the two spectrometers. The system magnification from target chamber center to the streak camera photocathode is 2.0 for the IAW and 2.7 for the EPW. Preceding the telescope is a MgF₂ blast window (100 mm diameter x 8 mm thick) which blocks particulate debris emanating from the laser target interaction during the shot. Figure 2 describes the telescope.

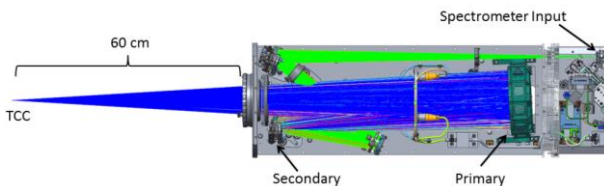


FIG. 2 The OTS f/8.3 telescope assembly contains a MgF₂ blast shield, off-axis Schwarzschild telescope and an off-axis parabolic mirror to deliver the light to the spectrometer.

B. Spectrometer System

The spectrometer group contains two Czerny-Turner type spectrometers that disperse the Thomson scattered light into two distinct bands, the IAW band and the EPW band. The spectrometers share the same 135 μm diameter input aperture pinhole (50 μm in the target image plane) and disperses the bands following a beam splitter that separates the light into two wavelength groups. The deep UV band 150-200 nm reflects off the front surface and the near UV band 206-214 nm passes through the splitter. Table 1 lists the associated design values for the optical system. Figure 3 shows the engineering model of the spectrometer group.

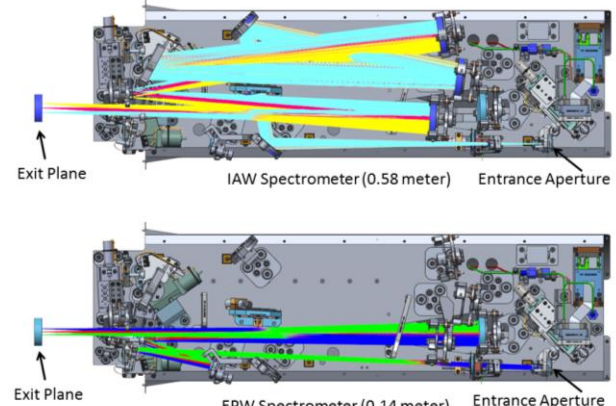


FIG. 3 The OTS spectrometer assemblies containing the IAW and EPW Czerny-Turner type spectrometers. The top image describes the IAW light path and the bottom image describes the EPW light path. The measurements are made simultaneously.

Table 1 Spectrometer design specifications for the optical Thomson scattering system

Specification	IAW	EPW
Spectrometer size (meter)	0.58	0.14
Spatial extent at photocathode (mm)	20	20
Desired bandwidth (nm)	4 ^a	50
Wavelength band (nm)	206-214	150-200
Spectrometer resolution ($\delta\lambda/\lambda$)	0.0001	0.01
Nominal grating spacing (gr/mm)	2400	1200
Grating order	2	1
Minimum dispersion at photocathode (nm/mm)	0.2293	4.437
Time resolution (ps)	200	200

^aThe 4 nm band is smaller than the full band. The grating will be adjusted to record any 4 nm band in the overall specified wavelength band.

III. DATA RECORDING

The Thomson scattering spectra will be recorded using an optical streak camera (Photonis, Inc. P510 sealed streak tube with an S20 photocathode deposited on a CaF₂ window). The measured quantum efficiency is 8% for the S20 photocathode at 150nm. The detector quantum efficiency will be measured upon completion of the diagnostic. The streak tube is driven by four selectable sweep windows that range from 3 ns to 45 ns. The data from the two spectrometers is recorded in the same sweep window with the IAW spectral content arriving approximately 5 ns later than the EPW spectral content. The spectrometers are designed to generate their dispersion bands over a 20-mm wide region in the spatial direction of the streak tube. The nominal resolution element of the recording system at the photocathode is 100 μm which defines the total number of recording elements as 200. The volume between the airbox window and the cathode window is filled with nitrogen to allow the deep-UV wavelengths to propagate from the airbox window to the cathode window with

minimal absorption. Figure 4 shows the optical streak camera assembly mounted in a DIM airbox.

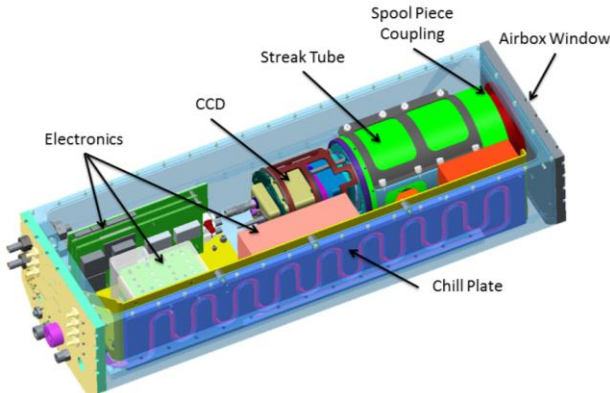


FIG 4. The optical Thomson scattering airbox and streak camera. The airbox input window is a CaF_2 and is coupled to a nitrogen gas tube that allows for deep UV light propagation to the input window of the streak tube.

The response from a NIF hohlraum target has been simulated using the expected system throughput, quantum efficiency and estimated background levels. The synthetic data described in figure 5 shows the temporal separation between the EPW and IAW spectrometers and their nominal wavelength band.

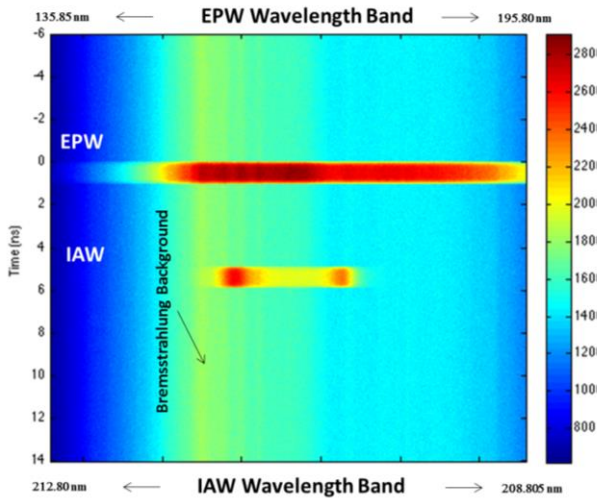


FIG 5. Phase-II simulated optical Thomson scattering data as expected over a 20 ns time window. The data includes quantum efficiency, background levels, the expected noise levels and expected system throughput.

IV. ALIGNMENT EFFICIENCY

The diagnostic is aligned to various targets using 660 nm laser diode illumination. An insertable pickoff mirror just before the spectrometer entrance pinhole directs light to an alignment CCD conjugate to the pinhole plane to ensure the Thomson volume is correctly imaged (or in focus). Dispersion from the diagnostic blast window causes the plane of best focus to vary with wavelength. For an 8 mm MgF_2 blast window, the shift is $\sim 411 \mu\text{m}$ from the 660 nm best focus to 150 nm best focus. Near the plane of best focus, the system is near diffraction-limited and the collection efficiency through the pinhole is very high ($\sim 96\text{-}98\%$). The collection efficiency of the system at the pinhole decreases away from the best focus. This “best focus” is

wavelength-dependent. The yellow band in figure 6 describes the offset of best focus relative to 210 nm for different wavelengths. The color scale describes the collection efficiency for different wavelengths as a function of defocus. Thus, during Phase I (background measurements, no probe), the effect of the dispersion is to collect the background measurements more efficiently from different depths of the plasma. In Phase II operation, the Thomson scattered light is only emitted from the volume where the probe laser is focused. To optimize the collection efficiency for a particular wavelength, the location of probe focus must coincide with the best focus for the wavelengths that are collected in each shot.

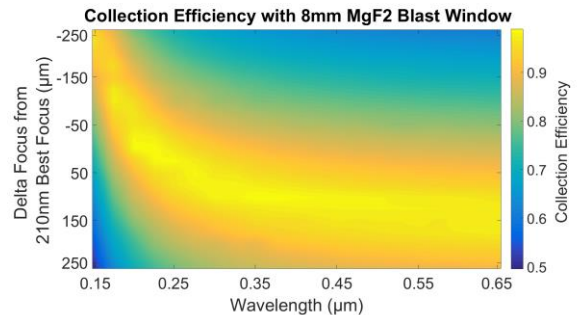


FIG 6. Plot representing the collection efficiency through the OTS spectrometer entrance aperture for different wavelength bands as a distance from best focus for a specific wavelength (210 nm). The OTS alignment laser diodes are 660 nm and is out of band for the measurement window.

V. CONCLUSION

The optical Thomson scattering diagnostics design is complete and is targeted to be installed into the NIF in the coming months. The goal of the first measurements is to measure the background from various target configurations that will establish signal-to-background limits, and provide guidance to the minimum energy of the probe laser that will be required in the Phase II implementation.

VI. ACKNOWLEDGMENTS

*This work performed under the auspices of the U.S. Department of Energy by Lawrence Livermore National Laboratory under Contract DE-AC52-07NA27344.

VII. REFERENCES

- ¹S. Glenzer, *et al.*, Phys. Rev. Lett. 79, 1277 (1997).
- ²D. H. Froula, J. S. Ross, L. Divol and S. Glenzer, Review of Scientific Instruments 77, 10E522 (2006).
- ³G. Miller, E. I. Moses and C. R. Wuest, Opt. Eng. 43, 2841 (2004).
- ⁴J. S. Ross, L. Divol, D. H. Froula and S. H. Glenzer, Journal of Instrumentation 6, P08004 (2011).
- ⁵J. Katz, R. Boni, C. Sorce, C. Follett, M. J. Shoup III and D. H. Froula, Review of Scientific Instruments 83, 10E349 (2012).
- ⁶P. Datté, G. James, P. Celliers, D. Kalantar, G. Vergel de Dios, Proc. SPIE Target Diagnostics Physics and Engineering for Inertial Confinement Fusion IV 95910D1 (2015).
- ⁷P. Datté, *et al.*, 9th International Conference on Inertial Fusion Sciences and Applications (IFSA), Journal of Physics: Conference Series 717, 012089 (2016).
- ⁸A. Visco, R. P. Drake, D. H. Froula, S. H. Glenzer and P. P. Pollock, Review of Scientific Instruments 79, 10F545 (2008).